Dev Genes Evol (2012) 222:125–138
DOI 10.1007/s00427-012-0394-8

ORIGINAL ARTICLE

A cellular network of dye-coupled glia associated with the embryonic central complex in the grasshopper *Schistocerca gregaria*

George S. Boyan · Yu Liu · Michael Loser

Received: 9 December 2011 / Accepted: 11 March 2012 / Published online: 30 March 2012
© Springer-Verlag 2012

Abstract The central complex of the grasshopper (*Schistocerca gregaria*) brain comprises a modular set of neuropils, which develops after mid-embryogenesis and is functional on hatching. Early in embryogenesis, Repo-positive glia cells are found intermingled among the commissures of the midbrain, but then redistribute as central complex modules become established and, by the end of embryogenesis, envelop all midbrain neuropils. The predominant glia associated with the central body during embryogenesis are glutamine synthetase-/Repo-positive astrocyte-like glia, which direct extensive processes (gliopodia) into and around midbrain neuropils. We used intracellular dye injection in brain slices to ascertain whether such glia are dye-coupled into a communicating cellular network during embryogenesis. Intracellular staining of individual cells located at any one of four sites around the central body revealed a population of dye-coupled cells whose number and spatial distribution were stereotypic for each site and comparable at both 70 and 100 % of embryogenesis. Subsequent immunolabeling confirmed these dye-coupled cells to be astrocyte-like glia. The addition of *n*-heptanol to the bathing saline prevented all dye coupling, consistent with gap junctions linking the glia surrounding the central body. Since dye coupling also occurred in the absence of direct intersomal contacts, it might additionally involve the extensive array of gliopodia, which develop after glia are arrayed around the central body. Collating the data from all injection sites suggests that the developing central body is surrounded by a network of dye-coupled glia, which we speculate may function as a positioning system for the developing neuropils of the central complex.

Keywords Insect · Embryo · Brain · Central complex · Glia

Communicated by S. Roth

Electronic supplementary material The online version of this article (doi:10.1007/s00427-012-0394-8) contains supplementary material, which is available to authorized users.

G. S. Boyan (✉) · Y. Liu · M. Loser
Developmental Neurobiology Group, Biocenter,
Ludwig-Maximilians-Universität,
Grosshadernerstrasse 2,
82152 Martinsried, Germany
e-mail: george.boyan@lmu.de

Introduction

The central complex in both the grasshopper and *Drosophila* comprises a set of highly structured neuropils (protocerebral bridge, central body, ellipsoid body, noduli, and lateral accessory lobes) whose role in sensory/motor coordination (Strauss 2002; Heinze and Homberg 2007; Strausfeld 2009) and spatial memory and orientation (Liu et al. 2006; Neuser et al. 2008) is well documented. In the grasshopper, this complex is functional at the time of hatching and so must develop during embryogenesis (see Boyan and Reichert 2011), whereas in holometabolous insects such as *Drosophila*, the equivalent modules arise during late larval stages and are thus first functional in the adult (Renn et al. 1999; Pereanu and Hartenstein 2006; Hartenstein et al. 2008; Izergina et al. 2009; Young and Armstrong 2010a, b; Pereanu et al. 2011). Comparative studies show that despite these different lifestyles, the central complex modules are generated by an equivalent set of progenitors (see Boyan and Reichert 2011) whose lineages contain both neurons and glia (Ito et al. 1997; Izergina et al. 2009; Boyan et al. 2010a,b; Viktorin et al. 2011).

Glia have been shown to play a major regulatory role in establishing neuroarchitecture throughout the insect nervous system (for reviews, see Hidalgo 2003; Klämbt 2009). Of the several types of glia known (for overviews, see Hoyle

1986; Jones 2001; Edwards and Meinertzhagen 2010), those that compartmentalize brain neuropils (Oland and Tolbert 1987, 1989; Breidbach et al. 1992; Hähnlein and Bicker 1996, 1997; Oland et al. 1999; Pereanu et al. 2005; Awasaki et al. 2008; Awasaki and Lee 2011; Boyan et al. 2011) are of especial interest to studies of central complex development. To this group belong astrocyte-like glia, which in vertebrates are implicated in glutaminergic synaptic transmission (van der Hel et al. 2005; Takahashi et al. 2010), and in the insect have extensive dendritic projections (or gliopodia) directed into neuropilar regions such as the central complex (Awasaki et al. 2008; Awasaki and Lee 2011; Boyan et al. 2011), a structure which in the grasshopper exhibits glutaminergic receptors (Homberg 2002).

Our interest was to determine whether glia of the central complex of the grasshopper *Schistocerca gregaria* communicate during development. To this end, we tested for dye coupling among immunolabeled (glutamine synthetase-positive/Repo-positive) astrocyte-like glia associated with the central complex at a stage when this neuropil was forming (70 % of embryogenesis) and again just prior to hatching (100 % of embryogenesis). Dye injected into a single glial cell at any one of four selected sites around the central body was seen to reliably spread to a population of neighboring glia cells whose number and spatial distribution were stereotypic for each site and highly comparable at both embryonic stages. The addition of *n*-heptanol to the bathing saline prevented all dye coupling, consistent with these glia communicating via gap junctions. Collating the data from all sites suggests that the developing central body is likely to be surrounded by a network of such dye-coupled glia. The network might function as a positioning system delimiting the developing neuropils of the central complex within the brain.

Materials and methods

Animals

S. gregaria eggs from our own culture were incubated in moist aerated containers at 30 °C. Embryos were staged at time intervals equal to percentage of embryogenesis according to Bentley et al. (1979). All experiments were performed strictly according to the guidelines for animal welfare as laid down by the Deutsche Forschungsgemeinschaft.

Intracellular dye injection

Brain slices were prepared as follows. Staged embryos (100 % of embryogenesis) were dissected out of the egg into ice-cold 0.1 M phosphate-buffered saline (PBS) and freed from embryonic membranes. Prior to embedding, brains were placed in a 1 % methylene blue solution for 5 min to stain the brain surface and thus facilitate visual orientation of the brain within the frozen blocks for sectioning. Brains were shock frozen, unfixed, at (−20 °C) in 2-methylbutane, without sucrose, and sectioned horizontally with respect to the body axis on a Leica cm3050s cryostat. Trial and error led to 16 μm being selected as the optimum section thickness, allowing individual cells to be easily targeted for intracellular dye injection under differential interference contrast (DIC) optics and avoiding damaging primary glial processes. In order to standardize results, and so allow comparisons between preparations and across ages, only sections at mid-depth through the central body as viewed from anterior were selected for experimentation unless otherwise stated. Frozen sections were transferred onto frozen Superfrost® Plus (Menzel-Gläser) microscope slides and stored at −18 °C. No changes in tissue preservation or dye coupling could be discerned with storage time.

Intracellular staining of cells was performed in unfixed brain slices prepared as above. The slide with the still frozen brain slice was transferred to a fixed-stage microscope (Zeiss Axioskop 2) equipped with epifluorescence and DIC optics. The section was covered with physiological saline (150 mM NaCl, 3 mM KCl, 2 mM $CaCl_2$, 1 mM $MgSO_4$, 5 mM TES buffer, pH 7.0) at room temperature. DIC images and intracellular dye injection confirm that cells did not rupture at any stage of the process (see "Results"). Cells were impaled with low resistance (30–40 M∧) thin walled glass micropipettes containing in most cases a solution of 10 mM Alexa Fluor® 568 (Invitrogen) in 200 mM KCl. This Alexa fluorochrome was preferred over Alexa Fluor® 488 and Lucifer yellow (which also revealed dye coupling—see Fig. 4) because of its staining intensity and because its emission spectrum is sufficiently narrow so as to prevent spectral overlap with those of the secondary antibodies used in the subsequent immunohistochemistry (see below). Electrode tips were dipped into fetal calf serum acting as a lubricant to facilitate penetration and removal of the electrode from the target cell. Intracellular penetrations of target cells were monitored optically using a Zeiss ceramic x63 Achromat water immersion objective mounted on a Zeiss Axioskop 2 microscope, a 1.3-MP color charge-coupled device (CCD) camera (Scion Corp.), and Scion Visicapture™ software. Penetrations were exclusively of the cell soma to avoid damage to, and inadvertent staining of, projections from neighboring cells. The electrode holder was connected to the head stage of a Getting 5DC Amplifier with current passing facility via a virtual ground circuit. Cells were stained iontophoretically using constant hyperpolarizing current not exceeding 5 nA and the electrode remained in situ for documentation purposes. A fine chlorided silver wire acting as a reference electrode was placed in the physiological solution covering the preparation. The various neuropilar modules of the central complex

as well as the glia cells associated with them were identified optically in the section based on their location and appearance. Glial identity was subsequently confirmed via immunohistochemistry performed directly on the brain slices containing dye-injected cells still affixed to the Superfrost® Plus (Menzel-Gläser) microscope slides. For glutamine synthetase immunohistochemistry, fixation was in aqueous Bouin (picric acid 71 %, formaldehyde 24 %, and glacial acetic acid 5 %) for 2 h at room temperature. After washing in 0.1 M PBS, slices were covered with preincubation medium comprising 1 % normal horse serum, 0.1 % bovine serum albumin (BSA), PBT (1 % Triton X-100 in 0.1 M PBS, pH 7.4) for 2 h at room temperature to block unspecific binding sites. Slices were exposed to the glutamine synthetase antibody (see above) diluted 1:200 in the preincubation medium for 48 h at 4 °C in the dark.

Gap junctional blocker

Alexa Fluor® 568 has a small molecular weight (see Weber et al. 2004) so that its passage between cells might be mediated by gap junctions. This possibility was tested by adding 1×10^{-5} M *n*-heptanol (a proven gap junctional blocker; see Weingart and Bukauskas 1998; Juszczak and Swiergiel 2009; Boyan et al. 2011) to the TES buffer bathing the brain slice prior to a dye-injection experiment. The concentration used was selected following similar experiments involving gap junctional communication in the embryonic grasshopper brain (Boyan et al. 2011) and in intact, unfixed, *Hydra* (Chapman et al. 2010). The presence of a stained cell on all occasions showed that the injection of dye itself was not affected by the presence of *n*-heptanol.

Cobalt injection

Intracellular injection was of 200 mM cobalt chloride for 60 min via 100 ms depolarizing current pulses of 1–3 nA (50 % duty cycle) into glia cells from brain slices prepared as described above except that Fielden's saline (Fielden 1960) was used. On removal of the electrode, one drop of 20 % ammonium sulfide/2 ml saline was applied to the section for 10 min to precipitate the cobalt. The brain slice was then washed in saline, fixed in aqueous Bouin for 1 h, washed several times in 70 % alcohol, hydrated to distilled water, and the cobalt sulfide precipitate intensified according to Bacon and Altman (1977). Preparations were then covered with Permount and coverslipped for microscopy.

Immunolabeling

Staged embryos were dissected out of the egg into ice-cold 0.1 M PBS and freed from embryonic membranes. Brains were immersion fixed in 3.7 % paraformaldehyde overnight at 4 °C. Preparations were then embedded in 5 % agarose/PBS at 55–60 °C, the solution allowed to cool, and the resulting block serially sectioned on a Vibratome (Leica VT 1000S) at 50 μm thickness. Sections were collected and washed overnight in 0.1 M PBS at 4 °C. Sections were then freed from agarose, positioned onto Superfrost® Plus (Menzel-Gläser) microscope slides, and covered with preincubation medium comprising 1 % normal goat serum, 0.1 % BSA, and PBT (1 % Triton X-100 in 0.1 M PBS, pH 7.4) for 1 h at room temperature to block unspecific binding sites. Immunohistochemistry was performed directly on this sectioned material. Brain slices were exposed to primary antibodies for 48 h at 4 °C in the dark unless otherwise stated.

Antibody 8B7 The monoclonal antibody 8B7 recognizes the Akt2 isoform of protein kinase B. The Akt2 kinase has an N-terminal (PH-) domain, a central kinase domain, and a hydrophobic C-terminal domain with regulatory function. In grasshopper, the Akt2 kinase is expressed early in development in neuroblasts and their progeny, later in axonal projections (Seeger et al. 1993). The 8B7 primary antibody (gift of M. Bastiani) was diluted 1:200 in preincubation medium.

Antihorseradish peroxidase Horseradish peroxidase belongs to the cell surface glycoproteins, which include cell adhesion and signal molecules (Snow et al. 1987). In insects, the epitope is neuron specific (Jan and Jan 1982; Haase et al. 2001) and is not expressed by glia. The antihorseradish peroxidase (anti-HRP) primary antibody (Jackson ImmunoResearch) was diluted 1:200 in preincubating medium.

Anti-Repo The protein generated by the glial homeobox gene *reversed polarity* (*repo*) is limited to the nuclei of glial cells and its expression can be revealed using the anti-Repo primary monoclonal antibody (Mab 4a3; Halter et al. 1995; gift of G. Technau) diluted 1:500 in preincubation medium.

Anti-glutamine synthetase Glutamine synthetase (GS) catalyzes the conversion of ammonia and glutamate to glutamine (Wedler and Horn 1976). Its presence in astrocyte-like glia of the grasshopper brain has been previously documented (see Boyan et al. 2011). The glutamine synthetase antibody (BD Transduction Laboratories™, mouse anti-6/GS, Nr. 610518) was diluted 1:200 in the preincubation medium. For GS/Repo double-labeling, fixation was in 3.7 % paraformaldehyde for 20 min at room temperature.

Secondary antibodies

After exposure to the primary antibody, brain slices were washed thoroughly in 0.1 M PBS and then placed in preincubation medium (see above) to which the relevant secondary antibody [goat anti-mouse (GAM) and goat anti-rabbit

(GAR)] was added for 24 h at 4 °C as follows: for anti-8B7 (GAM-Cy3, Sigma, 1:150 dilution), for anti-Repo (GAR-Cy3, Sigma, 1:150 dilution), for anti-glutamine synthetase (DAM-Alexa 488, Invitrogen, 1:300 dilution), and for anti-HRP (GAR-FITC, Dianova, or GAR-Cy3, Sigma, 1:150 dilution). For double stainings (anti-Repo/anti-Glutamine synthetase, anti-Repo/anti-8B7, and anti-HRP/anti-glutamine synthetase) appropriate secondary antibodies were selected in each case so as to prevent cross-reactions. Sections were then washed overnight in 0.1 M PBS at 4 °C in the dark, covered with Vectashield® (Vector Laboratories) and coverslipped for microscopy. Specificity of each secondary antibody was confirmed by its application in the absence of the primary (in no case was a staining pattern observed).

Histology

4,6-Diamidino-2-phenylindole (DAPI, Sigma) is a cell permeable fluorescent probe, which binds to the minor groove of double-stranded DNA (Naimski et al. 1980). DAPI was diluted 1:100 in 0.1 M PBS. Brain slices were exposed to DAPI for 30 min at room temperature, and this was followed by six washing cycles each of 20 min duration in 0.1 M PBS.

Imaging

Optical sections of preparations were acquired with a Leica TCS SP5 confocal laser scanning microscope equipped with ×20 and ×63 oil immersion objectives. Fluorochromes were visualized on the confocal microscope using an argon laser with excitation wavelengths of 488 nm for Alexa® 488, 568 nm for Alexa® 568, 561 nm for Cy3, and 430–440 nm for DAPI. On the Zeiss Axioskop 2 fluorescence microscope, the injected Alexa® Fluor 568 was also excited at violet excitation wavelengths (430–440 nm) and captured at yellow/orange emission wavelengths (535 nm) as this allowed better definition of stained cells and considerably reduced background when the brain slice was simultaneously illuminated with transmitted light. Stacks of confocal images were collated using public domain software (Fiji), and only the contrast and resolution were subsequently altered. Overlays of fluorescence and DIC images were obtained with the Zeiss Axioskop 2 microscope via a 1.3 MP color CCD camera (Scion Corp.) using Scion VisicaptureTM software and subsequently processed with Canvas X™ software.

Terminology

Unless otherwise stated, the axes used for anatomical analysis in this study are neuraxes, not body axes. The top of the brain (in the head) is neurally anterior, the front of the brain is neurally ventral, the back of the brain is neurally dorsal, and the base of the brain is neurally posterior. Planes of section, however, refer to the body axis. Postembryonic developmental stages (instars) are referred to as P1, P2, etc. as applicable.

Results

Midbrain glia redistribute during embryogenesis

The central complex develops during the latter half of embryogenesis. Prior to this (<50 %), Repo-positive glia of the midbrain are found distributed among 8B7-positive commissural fascicles (Fig. 1a). Subsequently (60 %), these midbrain glia redistribute and, for example, become associated with the early columnar neuroarchitecture of the emerging central body (Fig. 1b). As the central body (CB) neuroarchitecture matures (80 %), glial somata now surround this neuropil, thus compartmentalizing it from other brain structures (Fig. 1c). This glial distribution pattern is maintained through subsequent development (see Fig. 9).

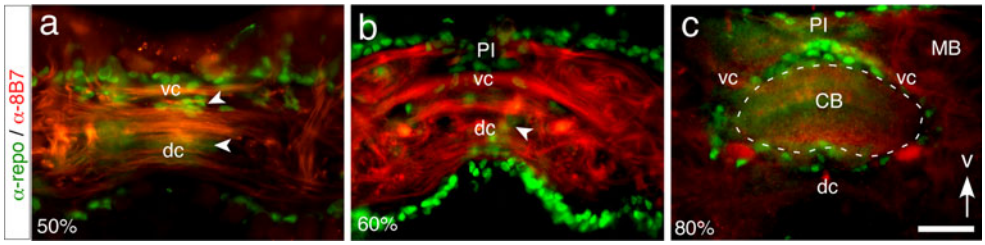

Fig. 1 Glia redistribute within the midbrain during embryogenesis. Photomicrographs of brain slices at three embryonic ages (50, 60, and 80 %) following double-labeling for glia (anti-Repo, *green*) and axons (anti-8B7, *red*). **a** Prior to formation of the central complex (50 %), glia surround brain neuropil and are found distributed between commissural fascicles of the midbrain (*white arrowheads*). **b** At 60 %, midbrain glia become associated with the columnar neuroarchitecture of the emerging central complex (*white arrowhead*). **c** As the central body (CB) forms (80 %), midbrain glia surround this neuropil (*outlined dashed white*), thus compartmentalizing it from other brain structures. *dc* dorsal commissures, *MB* mushroom body neuropil, *PI* pars intercerebralis, *vc* ventral commissures. *Arrow* points to ventral according to neuraxis. Scale bar in **c** represents 60 μm throughout

Astrocyte-like glia but not neurons surround the central body neuropil

Double-labeling reveals that GS-positive/HRP-negative cells (Fig. 2a, c) surround embryonic central complex neuropils such as the central body (CB). Furthermore, all these GS-positive cells are also Repo-positive (Fig. 2d). Based on this expression profile, the cells can be categorized as being astrocyte-like glia (see Boyan et al. 2011). HRP-positive neuronal somata, by contrast, are found in cortical regions such as the pars intercerebralis (PI), their axon projections within the CB, but no neuronal somata are located in the region immediately surrounding the CB (Fig. 2b). Since only very few Repo-positive/GS-negative cells appear to be present (Fig. 2d), we conclude that the great majority of glia surrounding the CB, and where intracellular dye injections were undertaken, are of the GS-positive/astrocyte-like type. As an additional control, the glial identity of dye-injected cells was independently confirmed after each experiment (see below).

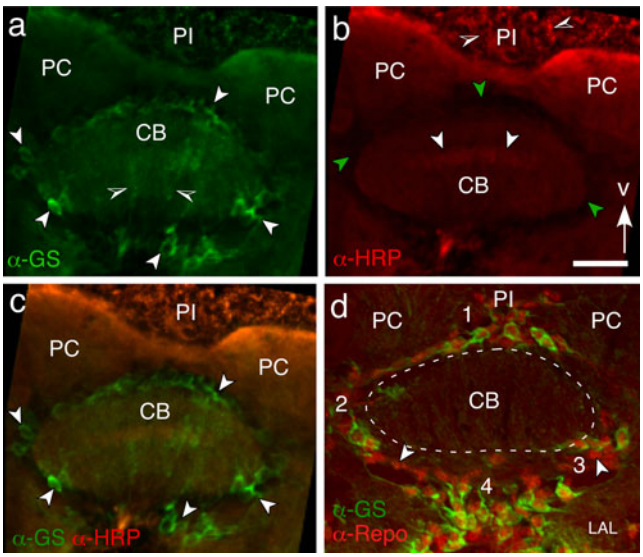

Fig. 2 Glia compartmentalizing central complex neuropils at the end of embryogenesis (100 %) are predominantly astrocyte-like. **a–c** Confocal images of a brain slice following double labeling for antiglutamine synthetase (GS, *green*) and anti-HRP (*red*). Separate channels (*red*/*green*) are viewed in **a** and **b**. **a** Green channel only. Immunolabeling reveals GS-positive astrocyte-like glia (*white arrowheads*) surrounding the central body (CB) and directing extensive projections (*open/white arrowheads*) into its neuropil. Note sparsity of GS-positive profiles in the pars intercerebralis (PI). **b**. Red channel only. Anti-HRP immunolabeling reveals band of HRP-positive neurites (*white arrowheads*) within the CB, as well as numerous HRP-positive somata (*open*/*white arrowheads*) within the PI. Note absence of HRP-positive profiles in the zone immediately surrounding the CB (*green arrowheads*). **c** Combined channels (*red*/*green*) reveal cells surrounding the CB are GS-positive/HRP-negative (*open white arrowheads*) and therefore astrocyte-like glia. **d** Confocal image of a brain slice following double immunolabeling (anti-Repo/anti-GS) reveals all GS-positive astrocyte-like glia (*green*) also coexpress anti-Repo (*red*). Other unidentified glia types (*white arrowheads*) are Repo-positive/GS-negative. *Numbers* represent the sites at which cells were intracellularly injected with dye to test for dye coupling (c.f. Fig. 3). *LAL* lateral accessory lobe, *PC* protocerebrum. *Arrow* points to ventral according to neuraxis. Scale bar in **b** represents 38 μm in **a–c**, 33 μm in **d**

Pattern of dye coupling at 100 % (prior to hatching)

As shown above (see Fig. 1), central complex neuropils, such as the central body, form during the latter half of embryogenesis, and by the 80 % stage, the glial distribution around this neuropil already has an adult-like character (see Fig. 9; Boyan et al. 2011). We therefore chose the 100 % stage just prior to hatching to initially test whether these glia were linked via dye coupling. We chose cells located at four sites with respect to central complex neuroarchitecture for intracellular injection (Fig. 2d). Site 1 lies between the central body neuropil and the PI—a region where migrating glia have been identified (Boyan et al. 2011); site 2 lies between the highly structured central body neuropil and that of the so-called diffuse neuropil more lateral in the protocerebrum; site 3 lies between the central body neuropil and that of the lateral accessory lobe (LAL); and site 4 lies dorsally between the CB, the ellipsoid body (EB) and/or the more posterior noduli (N).

Intracellular injection of Alexa® 568 fluorochrome into individual cells surrounding the CB revealed a population of dye-coupled cells at each of the four locations tested (Figs. 2d, 3). Dye coupling was observed using Alexa® 568, Alexa® 488, and Lucifer yellow fluorochromes, although Alexa® 568 was by far the most convincing fluorochrome based on the rate of dye spreading, the intensity of the staining, and its retention in stained cells. Dye injections were performed 31 times, and dye coupling was observed on 25 occasions (81 %). In each experiment, the cell chosen for injection was selected at random from within the population visible with DIC optics at each site. On those occasions where dye coupling failed, a repeat penetration was performed elsewhere in the same brain slice and was invariably positive for dye coupling. Such failures may be due to dye coupling never having been established among the cells tested or that an uncoupling has occurred at some earlier stage.

For each site tested, our data include a photomicrograph (DIC optics) showing the glass capillary located in the cell selected for staining (Fig. 3a, e, i, m), and then the staining present on initiation of current injection (0 min) (Fig. 3b, f, j, n), again after 3 min (Fig. 3c, g, k, o), and finally after 10 min (Fig. 3d, h, l, p) of dye injection. Dye injection was continuous, and where successful, dye began to spread from the injected cell to its neighbors within 3 min. The coupling pattern present after 10 min did not change with longer dye injection. Closer examination of the data reveals several

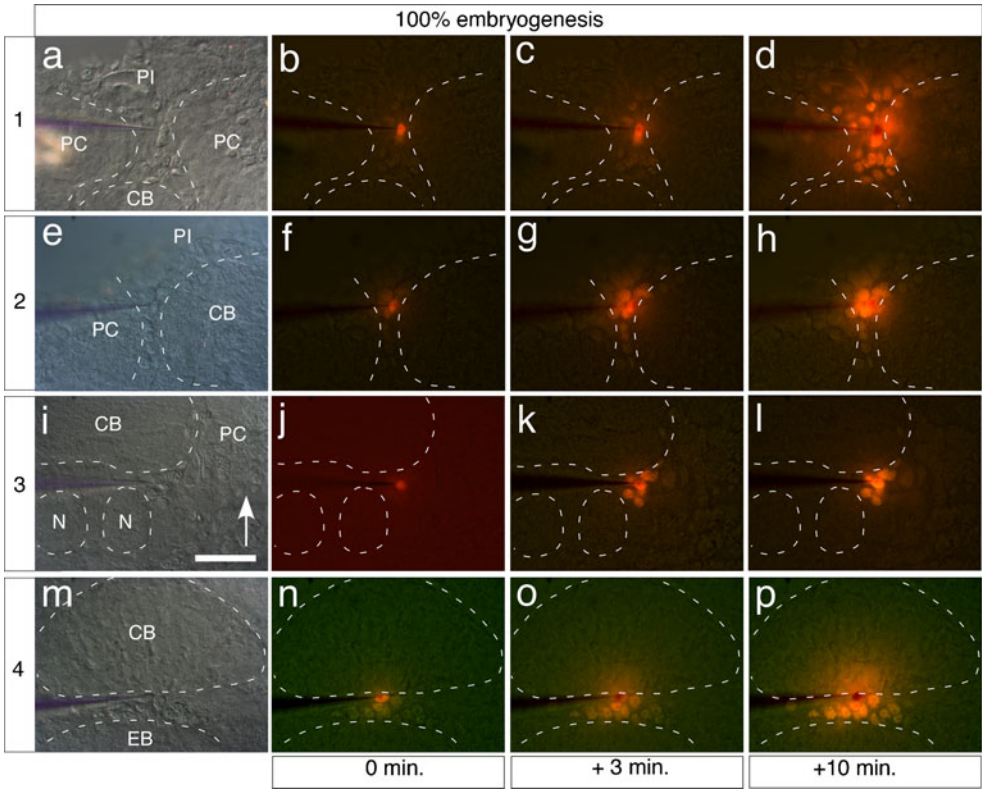

Fig. 3 Dye coupling between putative glia following intracellular injection of Alexa® Fluor 568 into single cells at four sites (*labeled 1–4*) surrounding the central body (CB) in brain slices at 100 % of embryogenesis. Glass capillary remained in place for the duration of the experiment. Photomicrographs were made on initial penetration of the cell (DIC: **a**, **e**, **i**, **m**), on commencement of dye injection (0 min., **b**, **f**, **j**, **n**), at +3 min (**c**, **g**, **k**, **o**) and again at the completion of the experiment (+10 min, **d**, **h**, **l**, **p**). Dye injection was continuous over this period. A cluster of dye-coupled cells with a configuration stereotypic for each site appears during the course of dye injection. Neuropilar regions are outlined (*dashed white*), and labeling in the DIC panels (**a**, **e**, **i**, **m**) also applies to the other images from each respective site. Fluorescence images are non-confocal photomicrographs. Simultaneous background illumination via transmitted light is used to reveal non-dye-coupled cells at each site, which leads to the slight color differences between image sets. Fluorescence images were taken using UV filter settings, which decreases the background but renders the Alexa® 568 fluorochrome orange. *EB* ellipsoid body, *N* nodule, *PC* protocerebrum, *PI* pars intercerebralis. *Arrow* in **i** indicates ventral according to the neuraxis, the scale bar represents 73 μm throughout

features of dye coupling: (a) the DIC images (Fig. 3a, e, i, m) show the cells from frozen, unfixed, brain slices to be intact, and for tissue preservation to be comparable to that found in slices following alternative histological fixation and staining methods (see Boyan et al. 2011); (b) the intracellular electrode was still in place at the completion of each experiment (Fig. 3d, h, l, p), which precluded an uncontrolled injection of dye into neighboring cells; and (c) stained cells could be several somal diameters distant from the injected cell and separated from it by unstained cells. These data suggest firstly that dye transfer via intersomal contact is not the only means of coupling and secondly argue against staining being due to a leaking of injected dye. To control for such a general extracellular "wash over" effect, dye was injected into the extracellular space immediately surrounding a small cluster of glia cells. The dye was not taken up by any cell of the cluster or by any neighboring cells (see Fig. 10 in the supplementary materials). Additionally, when a proven gap-junctional blocker was added to the bathing medium, the dye did not leak from the injected cell and no other cells were stained (see below).

The pattern of dye coupling we observed at the equivalent site in repeated experiments appears sufficiently consistent and sufficiently different from that seen at other sites (except for sites 2 and 3, which are very similar), as to suggest that distinct subpopulations of glia are involved (Fig. 4a). Dye-coupled glia at sites 2 and 3 appear more compactly organized than at sites 1 and 4 where extended arrays are present. This may relate to the anatomical features existing at each site (Fig. 2d). Site 1 lies ventral to the CB and extends into the PI, which is an expansive cortical region; sites 2 and 3 are sandwiched between the CB and the neighboring protocerebral neuropil; and site 4 lies dorsal to the CB and cells can extend laterally to either side but are bounded further dorsally by commissural fibres, by the ellipsoid body (EB), and more posteriorly by the noduli.

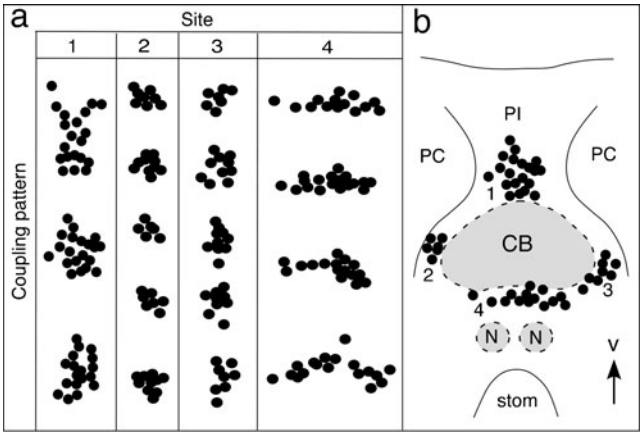

Fig. 4 Pattern of dye-coupled cells surrounding the CB at 100 % of embryogenesis as revealed by intracellular injection of Alexa® Fluor 568 into a single cell at each of the four sites (sites 1–4) tested. **a** *Black dots* represent stained cells (not to scale), and patterns were derived from overlays of fluorescence photomicrographs such as in Fig. 3 above. Cell clusters in each column represent the results of three repeat experiments at site 1, five repeat experiments at each of sites 2 and 3, and four repeat experiments at site 4. Differences in alignment between experiments at a given site reflect slight differences in the orientation and section plane of the original brain slice. **b**. Drawing of the midbrain region (semi-schematic) from an actual horizontal brain slice superimposed with representative clusters of dye-coupled cells from injection experiments at sites 1–4 as collated from different preparations. *Arrow* indicates ventral according to the neuraxis

Coupled cell numbers at each site also differ (Table 1). Comparisons of dye-coupled cell numbers from 20 experiments reveal that a mean of 19 cells (range, 18–20; n=3) were coupled at site 1; a mean of 7 cells (range, 4–10, n=8) were coupled at site 2; a mean of 9 cells (range 7–10, n=5) were coupled at site 3; and a mean of 17 cells (range, 14–18, n=4) were coupled at site 4. The sample sizes are too small to allow statistically meaningful conclusions to be drawn, but these data support the visual impression of a regulated flow of dye from cell to cell so that the coupling pattern is stereotypic for each recording site.

A further factor to consider relates to the extent to which fields of coupled cells might overlap and what this might mean for information processing in the glial cellular network. In the experiments reported above, a single glia cell at one of four sites was injected with dye (Figs. 2d and 3). A montage of the dye-coupled cells stained at a series of sites surrounding the CB (Fig. 4b) suggests that additional dye-injection experiments conducted at intercalated sites would result in the populations of dye-coupled glia completely enveloping the CB. However, we cannot say if this population represents a single functional entity.

The 2D views of dye-coupled cells presented thus far do not allow an estimate to be made of what proportion of the total population of cells at a given site are dye-coupled. This issue was addressed by performing injections at a given site in two successive brain slices of the same preparation, providing an overall sample depth of 32 μm and then recording the total number of dye-coupled cells found. The representative sites chosen were sites 2 and 4 (see Fig. 2d). The results were then compared with confocal data generated from brain slices of approximate equal thickness (50 μm) and at the equivalent anatomical depth in the brain, following DAPI staining and 3D reconstruction, which allowed all cells present at each site to be visualized (Fig. 5). The number of dye-coupled cells recorded over the two successive brain slices was 14 cells at site 2 and 23 cells at site 4. The data collated from five preparations following DAPI staining show the mean number of cells at site 2 was 16.0 cells (SD±2.55), and at site 4 was 23.2 cells (SD±8.44). The figures for the two sets of results cannot be conclusive but at least suggest that the majority of cells present at each site is likely to be dye-coupled. If so, then the CB is effectively enveloped by a 3D network of dye-coupled cells.

Table 1 Comparison of the mean number of stained cells resulting from dye coupling following intracellular dye injection into an individual glia cell at each of four sites (1–4, see Fig. 4) around the central body at 70 and 100 % of embryogenesis

Age	Site			
	1	2	3	4
70 %	22 (20–25)	7 (6–8)	11 (0)	12 (11–12)
	n=3	n=4	n=2	n=2
100 %	19 (18–20)	7 (4–10)	9 (7–10)	17 (14–18)
	n=3	n=8	n=5	n=4

Range of values (in brackets) and number of observations (n) are given

Pattern of dye coupling at 70 % (during embryogenesis)

Our interest then turned to the question of when the pattern of dye coupling described above is established—just prior to hatching, or earlier during embryogenesis. We therefore repeated the experiments at the 70 % stage of embryogenesis, an age at which the central complex neuroarchitecture is emerging and glia are assuming the locations around this developing neuropil, which they will maintain into postembryonic development (cf. Fig. 1 and see Fig. 9).

Dye injection experiments were performed in 16 preparations and at the equivalent sites around the central body to those at 100 % (Fig. 6). Target cells in these brain slices had the same histological appearance as those at 100 % (cf. Fig. 3). After 5 min of continuous dye injection into a single cell, a population of dye-coupled cells appeared in 11 of these preparations (Fig. 6, Table 1). The pattern of dye coupling was stereotypic for a given site and almost identical to that found at 100 % (c.f. Figs. 3 and 4). Although the sample sizes are small, the cell numbers present in each dye-coupled cluster also appear similar to those at 100 % (Table 1). The success rate for dye coupling (69 %) was considerably less than that at

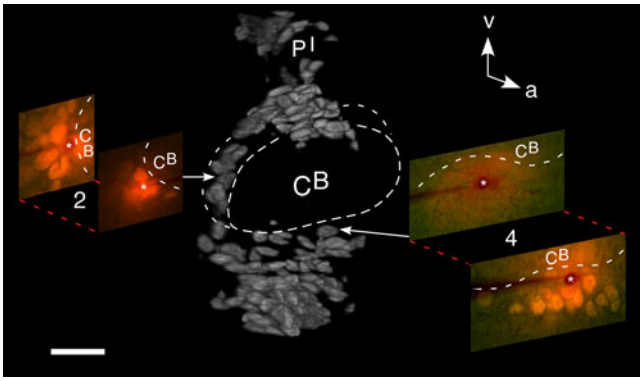

Fig. 5 Dye coupling incorporates most cells found at a given site around the central body at 100 % of embryogenesis. *Insets* show fluorescence photomicrographs from successive brain slices (*red dashed lines*, combined thickness 32 μm) at each of two sites (sites 2 and 4) associated with the central body (CB) of a given preparation. Injection of Alexa® Fluor 568 into a single cell (*white star*) revealed dye-coupled cells present in each slice. Dye-coupled data are compared (*white arrows*) with a confocal 3D view of a 50-μm brain slice taken at the same depth in the midbrain as for the dye injections but following DAPI staining to reveal the total cell population present at each site. Border of the CB is outlined (*dashed white*) throughout. Data from sites 2 and 4 are from different preparations. All images are in oblique view to provide a depth profile. Note that the more anterior image at location 4 forms part of the data set of Fig. 3. *Scale bar* represents 44 μm for photomicrographs with dye-injected cells, 29 μm for confocal image

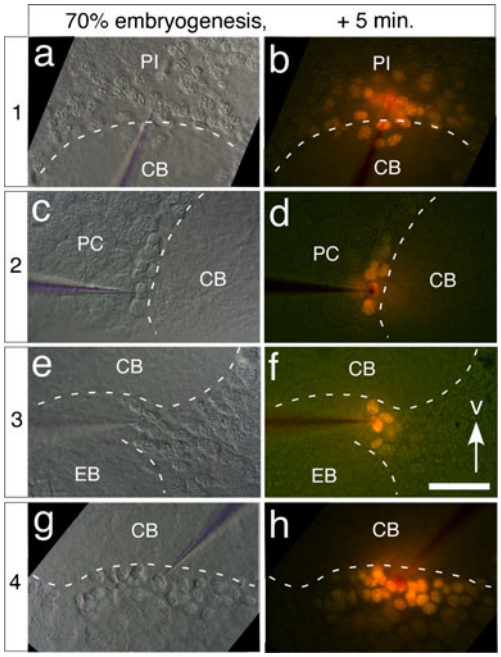

Fig. 6 Dye coupling between putative glia following intracellular injection of Alexa® Fluor 568 into single cells at four sites (*labeled 1–4*) surrounding the central body (CB) in brain slices at 70 % of embryogenesis. Injection sites, experimental conditions, and image acquisition are the same as described for the 100 % stage (cf. Fig. 3 above). Photomicrographs were made on initial penetration of the cell (DIC: **a**, **c**, **e**, **g**) and again at the completion of the experiment (+5 min., **b**, **d**, **f**, **g**). The cluster of dye-coupled cells has a configuration that is stereotypic for each site and almost identical to that reported at the 100 % stage (cf. Figs. 3 and 4). Neuropilar regions are outlined (*dashed white*). Fluorescence images are non-confocal photomicrographs. *PC* protocerebrum, *PI* pars intercerebralis. *Arrow* in **f** indicates ventral according to the neuraxis and the scale bar represents 60 μm throughout

100 % of embryogenesis (81 %), perhaps associated with the fact that 70 % of embryogenesis represents a developmental watershed at which central complex glia are first generating their gliopodia (cf. Fig. 9a, b). We therefore interpret the data as indicating that our sample included, on the one hand, preparations that were developmentally slightly more advanced, and so contained cells with more extensive gliopodial contacts, thus mediating the dye-coupling successes; on the other hand, preparations that were slightly less developmentally advanced and containing cells with few or no gliopodal contacts, thus leading to the failures.

Since glia only arrive at their locations around the central body at approximately 70 % of embryogenesis (c.f. Fig. 1), our data suggest that they are linked into a dye-coupled network or soon after this time. When we performed further dye injection experiments in preparations at 50 % of embryogenesis, we again found occasional groups of dye-coupled glia in the midbrain, but since the central complex is not formed at this stage, and we are unable to individually identify those cells that ultimately translocate to central complex modules, we did not pursue the analysis further.

Coupled cells are glia

Confirmation that dye-coupled cells are indeed glia was via immunolabeling subsequent to intracellular injection at both 70 % (Fig. 7a–c) and 100 % of embryogenesis (Fig. 7d–f). At 70 %, confocal analysis reveals a dye-injected cell from site 3 coupled to its neighbors (Fig. 7a). Immunolabeling reveals a cluster of GS-positive cells to be present at this site (Fig. 7b), and the combined images (Fig. 7c) show all injected cells to be GS-positive, confirming they are astrocyte-like glia. On repetition at 100 % of embryogenesis, three cells were separately impaled at location 4 (for reference see Fig. 2d) between the central body (CB) and noduli (N) (Fig. 7d) and injected with dye. Each was found to dye-couple to a number of neighboring cells (Fig. 7d). Immunolabeling with anti-GS revealed all the dye-coupled cells to also be GS positive (Fig. 7e), and the combined images (Fig. 7f) show a co-localization of Alexa® 568 and glutamine synthetase, confirming that both the injected and dye-coupled cells have an astrocyte-like glial identity.

Gap junctional blocker

Our initial controls (see Fig. 10, supplementary materials) showed that dye injected into extracellular space was not taken up by surrounding cells, consistent with dye coupling

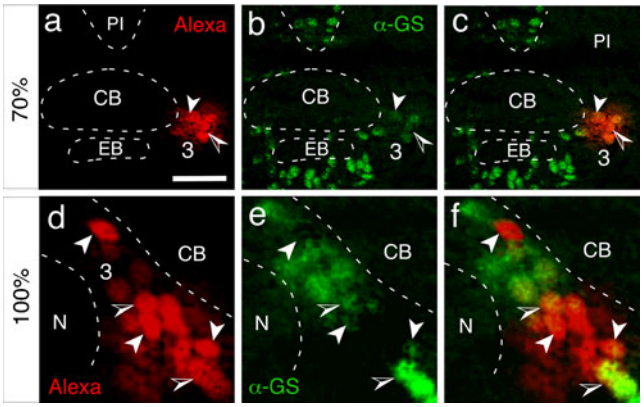

Fig. 7 Dye-coupled cells are astrocyte-like glia. Confocal images of brain slices at 70 % (**a–c**) and 100 % (**d–f**) of embryogenesis on injection of Alexa® Fluor 568 into single cells (*red channels*) and subsequent immunolabeling with anti-GS (*green channels*). **a** At 70 %, dye injection into a single cell (*white arrowhead*) at site 3 (c.f. Fig. 3) reveals a small cluster of dye-coupled cells (*open/white arrowhead*). **b** Immunolabeling (*green channel only*) reveals the cluster at site 3 to contain GS-positive astrocyte-like glia. *White arrowhead* points to dye-injected cell, *open/white arrowhead* to dye-coupled cells, from **a**. **c** Confocal image of the same brain slice as in **a**, **b** viewed with combined *red/green channels* shows the injected cell (*white arrowhead*) and the dye-coupled cells (*open/white arrowhead*) to also be GS-positive (*yellow*) and therefore astrocyte-like glia. **d** At 100 %, Alexa® Fluor 568 was injected into single cells (*white arrowheads*) at three locations within site 3 (*red channel only*). Dye-coupled cells (*open/white arrowheads*) are associated with the injected cells. **e** Immunolabeling (*green channel only*) reveals GS-positive astrocyte-like glia (e.g., *open/white arrowheads*) within the cluster at site 3. *White arrowheads* point to dye-injected cells from **d**. **f** Confocal image of the same brain slice as in **d**, **e** now viewed with combined *red/green channels* shows the injected cells (*white arrowheads*) and the dye-coupled cells (*open/white arrowheads*) to also be GS-positive (*yellow*) and therefore astrocyte-like glia. Scale bar in **a** represents 54 μm in **a–c**, 21 μm in **d–f**

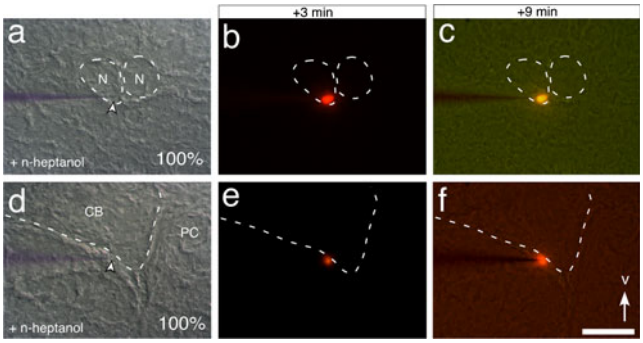

Fig. 8 *n*-Heptanol blocks dye coupling between glia associated with the central complex. Photomicrographs from two brain slices (**a–c**, **d–f**) at 100 % of embryogenesis following intracellular injection of Alexa® Fluor 568 into single glia from different sites with respect to central complex neuropils and in the presence of 1×10^{-5} M *n*-heptanol in the bathing medium. Photomicrographs were made on initial penetration of the cell (DIC: **a**, **d**), 3 min. after commencement of dye injection (**b**, **e**), and at the completion of the experiment (+9 min., **c**, **f**). The glass capillary remained in place throughout and dye injection was continuous. Varying background illumination with transmitted light accounts for color differences in the fluorescence images. No dye coupling to other neighboring cells occurred in the presence of *n*-heptanol. Arrow indicates ventral according to the neuraxis, and the scale bar represents 65 μm throughout

being mediated in a regulated way. The manner of dye transfer in our brain slices was revealed by applying the proven gap junctional blocker *n*-heptanol to the bathing saline (Fig. 8). Intracellular penetration of cells in repeated preparations—associated either with the noduli (Fig. 8a–c) or the central body (Fig. 8d–f)—followed by dye injection, revealed that even after 9 min of constant injection, the dye did not leak from the injected cell nor did the dye spread to any neighboring cells in the presence of *n*-heptanol. To control for the possibility of a failed dye-coupling experiment, cells at other locations in each brain slice were then impaled, but again, no dye coupling was observed. The data are consistent with dye coupling between the glia surrounding the CB being mediated via gap junctional communication, so that the dye-coupled cells belong to a cellular network.

Development of glial projections (gliopodia)

The injection experiments described above revealed that not all the somata of dye-coupled cells are in direct physical contact with one another (see Fig. 3). This suggests that dye coupling might also take place elsewhere such as through glial projections (gliopodia). That the astrocyte-like glia associated with the central complex later in embryogenesis do generate extensive projections, including into neuropils, can be demonstrated immunohistochemically (Fig. 9, inset i). That such gliopodia also contact one another, and that these contacts maybe involved in dye coupling, is evidenced by the network of projections linking coupled cells in the vicinity of the central body neuropil following intracellular injection of either Alexa® fluorochrome (Fig. 9, inset ii) or cobaltous chloride (Fig. 9 inset, iii) into a single cell soma at 100 % of embryogenesis.

When such projections arise during development was then established via immunolabeling at 70 % (Fig. 9a), 80 % (Fig. 9b), and 100 % (Fig. 9c) of embryogenesis and also at the first postembryonic instar (Fig. 9d). Reconstructions from confocal images show that at 70 % of embryogenesis (Fig. 9a), the majority of GS-positive/HRP-negative astrocyte-like glia located around the CB has yet to generate gliopodia. At 80 % of embryogenesis (Fig. 9b), most of the cells have sprouted processes, and these may infiltrate the CB itself or extend around it. By 100 % of embryogenesis (Fig. 9c), all the GS-positive/HRP-negative glia have generated gliopodia to a greater or lesser extent. This projection pattern is then maintained into postembryonic development (Fig. 9d).

Discussion

Glia of the invertebrate nervous system are involved in the formation of a blood–brain barrier (Schofield et al. 1984;

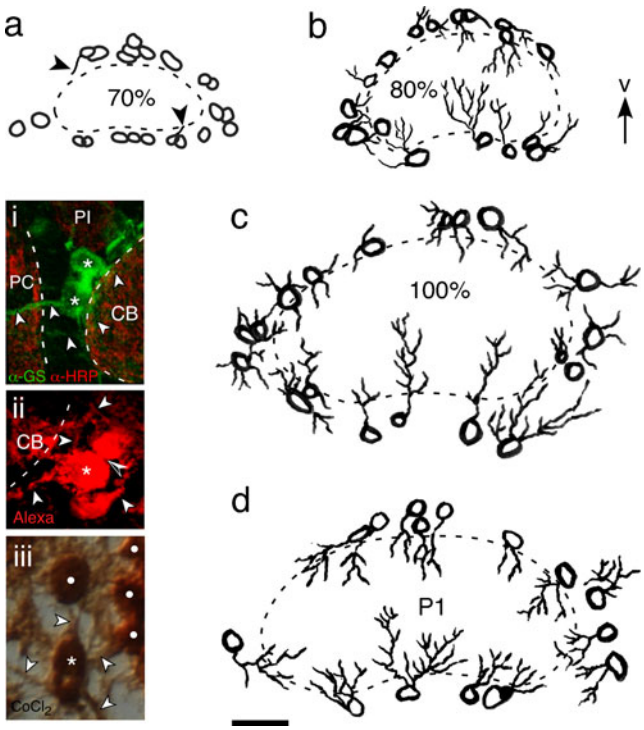

Fig. 9 Dendritic projections from astrocyte-like glia associated with the central body at four stages of development. Inset (*i*) is a confocal image of GS-positive/HRP-negative astrocyte-like glia (*white stars*) directing projections (*white arrowheads*) into central body (CB) and protocerebral (PC) neuropilar regions (*outlined dashed white*) of the midbrain at 100 % of embryogenesis. Inset (*ii*) is a confocal image of a cluster of dye-coupled glia at the border of the CB (*outlined dashed white*) following injection of Alexa® Fluor 568 into one of the cells (*white star*) at 100 % of embryogenesis. Stained gliopodia (*white arrowheads*) are evident, and cell somata are in contact (*open/white arrowhead*). Inset (*iii*) is a photomicrograph of a brain slice after intracellular injection of cobaltous chloride into a glia cell (*white star*) and subsequent silver intensification of the tissue at 100 % of embryogenesis. Note the network of stained projections (*white arrowheads*) linking coupled cells (*white dots*). Tissue preservation has unavoidably suffered from the intensification process. **a–d**. Drawings of GS-positive/HRP-negative astrocyte-like glia associated with the central body (*outlined dashed*) from confocal images of brain slices at 70 % of embryogenesis (**a**), 80 % of embryogenesis (**b**), 100 % of embryogenesis (**c**), and first postembryonic (P1) stage (**d**). *Arrowheads* in **a** point to initial gliopodial extensions. *Arrow* points to ventral. *Scale bar* represents 20 μm in inset **i**, 15 μm in insets **ii** and **iii**, 32 μm in **a–d**

Swales and Lane 1985; Carlson and Saint Marie 1990; Carlson et al. 2000; Pereanu et al. 2005; Banerjee and Bhat 2007), in phagocytic functions (Doherty et al. 2009), and in modulating synaptic transmission, for example, via K^+ and Ca^{2+} signaling (Schmidt and Deitmar 1996; Edwards and Meinertzhagen 2010; Koussa et al. 2010). Glial/neuronal interactions are also an integral component of insect nervous system development. Glia are a source of secreted cues for neuronal navigation and differentiation (see Silies and Klämbt 2011), they ensheath axons (Noordermeer et al. 1998), play a role in the commissural organization of the VNC (Tiemeyer and Goodman 1996; Page 2004), and, as a consequence of their own migration, glia can exert secondary effects on neuronal development (Bastiani and Goodman 1986; Jacobs and Goodman 1989; Fredieu and Mahowald 1989; Copenhaver 1993; Hidalgo and Booth 2000; Sepp and Auld 2003; Klämbt 2009; Silies and Klämbt 2011).

Dye coupling and gap junctions

The central complex of the grasshopper is functional on hatching, so that glia/glia and glia/neuronal interactions must not only be established, but reach considerable maturity, during embryogenesis (see Boyan and Reichert 2011). Prior to the formation of the central complex in the grasshopper, glia are initially found in the PI and distributed among the commissural fascicles of the grasshopper midbrain (Fig. 1a; Boyan et al. 2011). As the central complex becomes established, these glia migrate to envelop the emerging neuroarchitecture as previously reported for midline brain neuropils in a range of species (Nordlander and Edwards 1969; Vanhems 1985; Ito et al. 1994; Hähnlein and Bicker 1996, 1997; Hartenstein et al. 1998; Pereanu et al. 2005; Boyan et al. 2011). Migration of glia in the central and peripheral nervous system of insects has been shown to depend on both neuron/glia and glia/glia interactions (Rangarajaran et al. 1999; Silies et al. 2007; Klämbt 2009; Silies and Klämbt 2011). Among the factors playing a role in such glial interactions in the nervous systems of both insects (Koussa et al. 2010) and vertebrates (Parys et al. 2010) is Ca^{2+} signaling via gap junctions, and one indicator of gap junctional communication is the presence of dye coupling as revealed by fluorescent dyes (Hossain et al. 1995; Ball et al. 2007; Lanosa et al. 2008; Koussa et al. 2010).

In vertebrates, glia are known to communicate via gap junctions (Zahs and Newman 1997; Newman 2001; Rela et al. 2010) resulting in cellular networks that may comprise astrocytes alone (Theiss and Meller 2002; Houades et al. 2008; Tanaka et al. 2008), astrocytes and oligodendrocytes (Parys et al. 2010), or astrocytes and neurons (Hatton 2002; Schummers et al. 2008). In invertebrates, gap junctional communication has been reported between neurons (Wilcox 1994; Alexopolous et al. 2004; Dykes et al. 2004; Ducret et al. 2006) and between glia (e.g. Swales and Lane 1985; Schmidt and Deitmar 1996; Edwards and Meinertzhagen 2010) of several species and the molecular basis of electrical coupling in identified neuronal systems such as the giant fiber system of *Drosophila* examined (Phelan et al. 2008). The development of gap junctional communication specifically between glia has been investigated ultrastructurally in the ventral nerve cord of the embryonic grasshopper (Swales and Lane 1985). Gap junctions, tight junctions, and septate junctions have been shown to assemble in glial cells during the latter half of embryogenesis as a result of the lateral migration of so-called intramembranous particles (Swales and Lane 1985). The establishment of the resulting glial cellular network

coincides temporally with the onset of mature electrical properties (Goodman et al. 1979; Goodman and Spitzer 1981) and transmitter systems (Goodman et al. 1979; Goodman and Spitzer 1980) in the lineages of neurons with which the glia interact. Interestingly, electrical interactions in these same lineages earlier in embryogenesis are also mediated by gap junctional communication (Goodman et al. 1979; Goodman and Spitzer 1981).

In the brain, dye coupling has been demonstrated using both intracellular and extracellular markers in embryonic lineages generating the central complex: in wholemount, unfixed, embryonic brains (Ludwig et al. 1999; Boyan et al. 2008); fixed agarose-embedded brain slices (Boyan et al. 2011); and unfixed, frozen brain slices (Figs. 3 and 6). Prevention of dye coupling can be induced in both frozen and unfrozen brain tissues via *n*-heptanol (Fig. 8; Boyan et al. 2011), an acknowledged gap junctional blocker (Burt and Spray 1980; Weingart and Bukauskas 1998; Juszczak and Swiergiel 2009; Chapman et al. 2010). Unlike the segmental giant neuropil glial cells in the leech (Schmidt and Deitmar 1996), the glia associated with the central body in this study are not individually identifiable, so that even if equivalent cells were to be present in different preparations, we would not have been able to recognize them. Consequently, we almost certainly injected a different individual cell at a given location in each experiment. Nevertheless, the pattern and number of dye-coupled cells for each site tested was so similar at 70 and 100 % of embryogenesis (Figs. 3 and 6), and so different between sites, that coupling pattern could be said to match central body location independently of age. We can conclude from this that once migratory glia have assumed a particular location around the central body, the network of connections they establish soon after is then maintained during subsequent development.

A comparison of dye coupling found across more than one brain slice at a given site with 3D reconstructions of the total cell population at that site suggests that most of the cells present are likely to be dye-coupled (Fig. 5). Superimposing the patterns of staining from all sites shows that the central body neuropil would be completely enveloped by dye-coupled glial cells (Fig. 4b), although whether they form a unified network remains unclear. While our data are consistent with the existence of gap junctional communication between central complex glia, molecular or electron microscopical confirmation will ultimately be required because as shown for the fly visual system, not all gap junctions in electrically coupled cells allow dye coupling (Wilcox 1994).

Gliopodia and dye coupling during development

The fact that glia associated with the central complex need not be in direct somal contact for dye coupling to occur (Fig. 3) suggests that if gap junctions are responsible, these may be regionalized to both the soma and gliopodia. On translocating into the region surrounding the developing central body at around 60–70 % of embryogenesis (Fig. 1), our study shows that very few Repo-positive/GS-positive (astrocyte-like) glia have generated gliopodia (Fig. 9a). These glia must therefore migrate to their target as largely naked somata. Consistent with this anatomical finding, our microelectrode injection experiments at 70 % of development reveal a lower success rate of dye coupling than later. By 80 % of embryogenesis, gliopodal extension has markedly increased (Fig. 9b). Assuming that gap junctions are already in place and functional in midbrain glia by 70 %, as is the case in glia of the ventral nerve cord (Swales and Lane 1985), we speculate that the successful cases of dye coupling at 70 % were from preparations where sufficient gliopodia were already present to mediate the effect.

At the end of embryogenesis, the gliopodia from astrocyte-like glia ramify extensively throughout central complex neuropils (Fig. 9c; Boyan et al. 2011). This pattern is then maintained into postembryonic stages (Fig. 9d). In the case of the central body, gliopodia project onto its stereotypic columnar fiber system (Williams 1975; Heinze and Homberg 2008; el Jundi et al. 2010; Boyan and Reichert 2011; Boyan et al. 2011). Genetic ablation of embryonic glial cells is known to cause neuronal loss and neural wiring defects in *Drosophila* (Booth et al. 2000; Hidalgo and Booth 2000), and ablation experiments in the antennal lobe of *Manduca* show that the organization of glomeruli depends on interactions between neurites and migrating glia (Oland and Tolbert 1987, 1989; Oland et al. 1999). Furthermore, gliopodia generated by midline glia have been shown to contact neurites and for misexpression of Rac1N17 in these glia to downregulate gliopodia and so alter the position of midline neuropils in the ventral nerve cord of *Drosophila* (Vasenkova et al. 2006). It is an intriguing speculation that in the grasshopper, the cellular network of embryonic glia associated with the central complex may, as in *Drosophila*, function as a stereotactic positioning system regulating the position and extent of neuropils and, in this capacity, represent one element adapting such embryonic neuronal networks for postembryonic life (Stevenson and Kutsch 1986).

Acknowledgments We thank Dr. Les Williams for assistance with the silver intensification procedures, Karin Fischer for establishing protocols for producing the brain slices, and Ms. Stefanie Götz for criticisms of the manuscript. Grant sponsor: Deutsche Forschungsgemeinschaft (BO 1434/3-5).

References

Alexopoulos H, Böttger A, Fischer S, Levin A, Wolf A, Fujisawa T, Hayakawa S, Gojobori T, Davies JA, David CN, Bacon JP (2004)

Evolution of gap junctions: the missing link? Curr Biol 14:879–880

Awasaki T, Lee T (2011) New tools for the analysis of glial cell biology in *Drosophila*. Glia 59:1377–1386

Awasaki T, Lai S-L, Ito K, Lee T (2008) Organization and postembryonic development of glial cells in the adult central brain of *Drosophila*. J Neurosci 28:13742–13753

Bacon JP, Altman JS (1977) A silver intensification method for cobalt-filled neurones in wholemount preparations. Brain Res 138:359–363

Ball KK, Gandhi GK, Thrash J, Cruz NF, Dienel GA (2007) Astrocytic connexin distributions and rapid, extensive dye transfer via gap junctions in the inferior colliculus: implications for [^{14}C] Glucose metabolite trafficking. J Neurosci Res 85:3267–3283

Banerjee S, Bhat MA (2007) Neuron-glial interactions in blood–brain barrier formation. Ann Rev Neurosci 30:235–258

Bastiani MJ, Goodman CS (1986) Guidance of neuronal growth cones in the grasshopper embryo. III. Recognition of specific glial pathways. J Neurosci 6:3542–3551

Bentley D, Keshishian H, Shankland M, Torian-Raymond A (1979) Quantitative staging of embryonic development of the grasshopper, *Schistocerca nitens*. J Embryol Exp Morphol 54:47–74

Booth GE, Kinrade EFV, Hidalgo A (2000) Glia maintain follower neuron survival during *Drosophila* CNS development. Development 127:237–244

Boyan GS, Reichert H (2011) Mechanisms for complexity in the brain: generating the insect central complex. Trends Neurosci 34:247–257

Boyan GS, Williams JL, Herbert Z (2008) Fascicle switching generates a chiasmal neuroarchitecture in the embryonic central body of the grasshopper *Schistocerca gregaria*. Arthr Struct Dev 37:539–544

Boyan G, Herbert Z, Williams L (2010a) Cell death shapes embryonic lineages of the central complex in the grasshopper *Schistocerca gregaria*. J Morphol 271:949–959

Boyan G, Williams L, Legl A, Herbert Z (2010b) Proliferative cell types in embryonic lineages of the central complex of the grasshopper *Schistocerca gregaria*. Cell Tissue Res 341:259–277

Boyan G, Loser M, Williams L, Liu Y (2011) Astrocyte-like glia associated with the embryonic development of the central complex in the grasshopper *Schistocerca gregaria*. Dev Genes Evol 221:141–155

Breidbach O, Dennis R, Marx J, Görlach C, Wiegandt H, Wegerhoff R (1992) Insect glial cells show differential expression of a glycolipid-derived, glucuronic acid-containing epitope throughout neurogenesis: detection during postembryogenesis and regeneration in the central nervous system of *Tenebrio molitor* L. Neurosci Lett 147:5–8

Burt JM, Spray DC (1980) Single-channel events and gating behavior of the cardiac gap junction channel. Proc Natl Acad Sci U S A 85:3431–3434

Carlson SD, Saint Marie RL (1990) Structure and function of insect glia. Ann Rev Entomol 35:597–621

Carlson SD, Juang JL, Hilgers SL, Garment MB (2000) Blood barriers of the insect. Ann Rev Entomol 45:151–174

Chapman JA, Kirkness EF, Simakov O, Hampson SE, Mitros T, Weinmaier T, Rattei T, Balasubramanian PG, Borman J, Busam D, Disbennett K, Pfannkoch C, Sumin N, Sutton GG, Viswanathan LD, Walenz B, Goodstein DM, Hellsten U, Kawashima T, Prochnik SE, Putnam NH, Shu S, Blumberg B, Dana CE, Gee L, Kibler DF, Law L, Lindgens D, Martinez DE, Peng J, Wigge PA, Bertulat B, Guder C, Nakamura Y, Ozbek S, Watanabe H, Khalturin K, Hemmrich G, Franke A, Augustin R, Fraune S, Hayakawa E, Hayakawa S, Hirose M, Hwang JS, Ikeo K, Nishimiya-Fujisawa C, Ogura A, Takahashi T, Steinmetz PRH, Zhang X, Aufschnaiter R, Eder M-E, Gorny A-K, Salvenmoser W, Heimberg AM, Wheeler BM, Peterson KJ, Böttger A, Tischler P, Wolf A, Gojobori T, Remington KA, Strausberg RL, Venter JC, Technau U, Hobmayer B, Bosch TCG, Holstein TW, Fujisawa T, Bode HR, David CN, Rokhsar DS, Steele RE (2010) The dynamic genome of *Hydra*. Nature 464:592–596

Copenhaver PF (1993) Origins, migration and differentiation of glial cells in the insect enteric nervous system from a discrete set of glial precursors. Development 117:59–74

Doherty J, Logan MA, Tasdemir OE, Freeman MR (2009) Ensheathing glia function as phagocytes in the adult *Drosophila* brain. J Neurosci 29:4768–4781

Ducret E, Alexopoulos H, Le Feuvre Y, Davies JA, Meyrand P, Bacon JP, Fénelon VS (2006) Innexins in the lobster stomatogastric nervous system: cloning, phylogenetic analysis, developmental changes and expression within adult identified dye and electrically coupled neurons. Eur J Neurosci 24:3119–3133

Dykes IM, Freeman FM, Bacon JP, Davies JA (2004) Molecular basis of gap-junctional communication in the CNS of the leech *Hirudo medicinalis*. J Neurosci 24:886–94

Edwards TN, Meinertzhagen IA (2010) The functional organisation of glia in the adult brain of *Drosophila* and other insects. Prog Neurobiol 90:471–497

el Jundi B, Heinze S, Lenschow C, Kurylas A, Rohlfing T, Homberg U (2010) The locust standard brain: a 3D standard of the central complex as a platform for neural network analysis. Front Syst Neurosci 3:21

Fielden A (1960) Transmission through the last abdominal ganglion of the dragonfly nymph *Anax imperator*. J Exp Biol 37:832–844

Fredieu JR, Mahowald AP (1989) Glial interactions with neurons during *Drosophila* embryogenesis. Development 106:739–748

Goodman CS, Spitzer NC (1980) Embryonic development of neurotransmitter receptors in grasshoppers. In: Sattelle DB, Hall LM, Hildebrand JG (eds) Receptors for neurotransmitters, hormones and pheromones in insects. Elsevier/North-Holland Biomedical Press, Amsterdam, pp 195–207

Goodman CS, Spitzer NC (1981) The development of electrical properties of identified neurons in grasshopper embryos. J Physiol (Lond) 313:385–413

Goodman CS, O'Shea M, Caman R, Spitzer NC (1979) Embryonic development of identified neurons: temporal pattern of morphological and biochemical differentiation. Science 204:1219–1222

Haase A, Stern M, Wächtler K, Bicker G (2001) A tissue-specific marker of Ecdysozoa. Dev Genes Evol 211:428–433

Hähnlein I, Bicker G (1996) Morphology of neuroglia in the antennal lobes and mushroom bodies of the brain of the honeybee. J Comp Neurol 367:235–245

Hähnlein I, Bicker G (1997) Glial patterning during postemebryonic development of central neuropiles in the brain of the honeybee. Dev Genes Evol 207:29–41

Halter DA, Urban J, Rickert C, Ner SS, Ito K, Travers AA, Technau GM (1995) The homeobox gene repo is required for the differentiation and maintenance of glial function in the embryonic nervous system of *Drosophila melanogaster*. Development 121:317–322

Hartenstein V, Nassif C, Lekven A (1998) Embryonic development of the *Drosophila* brain. II. Pattern of glia cells. J Comp Neurol 402:32–47

Hartenstein V, Spindler S, Pereanu W, Fung S (2008) The development of the *Drosophila* larval brain. Adv Exp Med Biol 628:1–31

Hatton GI (2002) Glial-neuronal interactions in the mammalian brain. Adv Physiol Educ 26:225–237

Heinze S, Homberg U (2007) Maplike representation of celestial e-vector orientations in the brain of an insect. Science 315:995–997

Heinze S, Homberg U (2008) Neuroarchitecture of the central complex of the desert locust: intrinsic and columnar neurons. J Comp Neurol 511:454–478

Hidalgo A (2003) Neuron-glia interactions during axon guidance in *Drosophila*. Biochem Soc Trans 31:50–55

Hidalgo A, Booth GE (2000) Glia dictate pioneer axon trajectories in the *Drosophila* embryonic CNS. Development 127:393–402

Homberg U (2002) Neurotransmitters and neuropeptides in the brain of the locust. Microsc Res Tech 56:189–209

Hossain MZ, Ernst LA, Nagy JI (1995) Utility of intensely fluorescent cyanine dyes (Cy3) for assay of gap junctional communication by dye-transfer. Neurosci Lett 184:71–74

Houades V, Koulakoff A, Ezan P, Seif I, Giaume C (2008) Gap junction-mediated astrocytic networks in the mouse barrel cortex. J Neurosci 28:5207–5217

Hoyle G (1986) Glial cells of an insect ganglion. J Comp Neurol 246:85–103

Ito K, Urban J, Technau GM (1994) Distribution, classification and development of *Drosophila* glial cells during late embryogenesis. Roux's Arch Dev Biol 204:284–307

Ito K, Awano W, Suzuki K, Hiromi Y, Yamamoto D (1997) The *Drosophila* mushroom body is a quadruple structure of clonal units each of which contains a virtually identical set of neurones and glial cells. Development 124:761–771

Izergina N, Balmer J, Bello B, Reichert H (2009) Postembryonic development of transit amplifying neuroblast lineages in the *Drosophila* brain. Neural Dev 4:44

Jacobs JR, Goodman CS (1989) Embryonic development of axon pathways in the *Drosophila* CNS. I. A glial scaffold appears before the first growth cones. J Neurosci 9:2402–2411

Jan LY, Jan YN (1982) Antibodies to horseradish-peroxidase as specific neuronal markers in *Drosophila* and grasshopper embryos. Proc Natl Acad Sci U S A 79:2700–2704

Jones BW (2001) Glial cell development in the *Drosophila* embryo. BioEssays 23:877–887

Juszczak GR, Swiergiel AH (2009) Properties of gap junction blockers and their behavioural, cognitive and electrophysiological effects: animal and human studies. Prog Neuro-Psychopharm Biol Psychiat 33:181–198

Klämbt C (2009) Modes and regulation of glial migration in vertebrates and invertebrates. Nat Rev Neurosci 10:769–779

Koussa MA, Tolbert LP, Oland LA (2010) Development of a glial network in the olfactory nerve: role of calcium and neuronal activity. Neuron Glia Biol 6:245–261

Lanosa XA, Reisin HD, Santacroce I, Colombo JA (2008) Astroglial dye-coupling: an in vitro analysis of regional and interspecies differences in rodents and primates. Brain Res 1240:82–86

Liu G, Seiler H, Wen A, Zars T, Ito K, Wolf M, Heisenberg M, Liu L (2006) Distinct memory traces for two visual features in the *Drosophila* brain. Nature 439:551–556

Ludwig P, Williams JLD, Lodde E, Reichert H, Boyan GS (1999) Neurogenesis in the median domain of the embryonic brain of the grasshopper *Schistocerca gregaria*. J Comp Neurol 414:379–390

Naimski P, Bierzyimageski A, Fikus M (1980) Quantitative fluorescent analysis of different conformational forms of DNA bound to the dye 4´, 6-diamidine-2-phenylindole, and separated by gel electrophoresis. Anal Biochem 106:471–475

Neuser K, Triphan T, Mronz M, Poeck B, Strauss R (2008) Analysis of a spatial orientation memory in *Drosophila*. Nature 453:1244–1247

Newman EA (2001) Propagation of intercellular calium waves in retinal astrocytes and Müller cells. J Neurosci 21:2215–2223

Noordermeer JN, Kopczynski CC, Fetter RD, Bland KS, Chen W-Y, Goodman CS (1998) Wrapper, a novel member of the Ig superfamily, is expressed by midline glia and is required for them to ensheath commissural axons in *Drosophila*. Neuron 21:991–1001

Nordlander RH, Edwards JS (1969) Postembryonic brain development in the monarch butterfly, *Danaus plexippus plexippus*, L. I Cellular events during brain morphogenesis. Wilh Roux Árchiv 162:197–217

Oland LA, Tolbert LP (1987) Glial patterns during early development of antennal lobes of *Manduca sexta*: a comparison between normal lobes and lobes deprived of antennal axons. J Comp Neurol 255:196–207

Oland LA, Tolbert LP (1989) Patterns of glial proliferation during formation of olfactory glomeruli in an insect. Glia 2:10–24

Oland LA, Marrero HG, Burger I (1999) Glial cells in the developing and adult olfactory lobe of the moth Manduca sexta. Cell Tissue Res 297:527–545

Page DT (2004) A mode of arthropod brain evolution suggested by *Drosophila* commissure development. Evol Dev 6:25–31

Parys B, Cote A, Gallo V, De Koninck P, Sik A (2010) Intercellular calcium signaling between astrocytes and oligodendrocytes via gap junctions in culture. Neuroscience 167:1032–1043

Pereanu W, Hartenstein V (2006) Neural lineages of the *Drosophila* brain: a three-dimensional digital atlas of the pattern of lineage location and projection at the late larval stage. J Neurosci 26:5534–5553

Pereanu W, Shy D, Hartenstein V (2005) Morphogenesis and proliferation of the larval brain glia in *Drosophila*. Dev Biol 283:191–203

Pereanu W, Younossi-Hartenstein A, Lovick J, Spindler S, Hartenstein V (2011) A lineage-based analysis of the development of the central complex of the *Drosophila* brain. J Comp Neurol 519:661–689

Phelan P, Goulding LA, Tam JLY, Dawber RJ, Davies JA, Bacon JP (2008) Molecular mechanism of rectification at an identified electrical synapse in the *Drosophila* giant fibre system. Curr Biol 18:1955–1960

Rangarajan R, Gong Q, Gaul U (1999) Migration and function of glia in the developing *Drosophila* eye. Development 126:3285–3292

Rela L, Bordey A, Greer CA (2010) Olfactory ensheathing cell membrane properties are shaped by connectivity. Glia 58:665–678

Renn SCN, Armstrong JD, Yang M, Wang Z, An X, Kaiser K, Taghert PH (1999) Genetic analysis of the *Drosophila* ellipsoid body neuropil: organization and development of the central complex. J Neurobiol 41:189–207

Schmidt J, Deitmar JW (1996) Photoinactivation of the giant neuropil glial cells in the leech *Hirudo medicinalis*: effects on neuronal activity and synaptic transmission. J Neurophysiol 76:2861–2871

Schofield PK, Swales LS, Trehern JE (1984) Potentials associated with the blood–brain barrier of an insect: recordings from identified neuroglia. J Exp Biol 109:307–318

Schummers J, Yu H, Sur M (2008) Tuned responses of astrocytes and their influence on hemodynamic signals in the visual cortex. Science 320:1638–1643

Seeger M, Tear G, Ferres-Marco D, Goodman CS (1993) Mutations affecting growth cone guidance in *Drosophila*: genes necessary for guidance toward or away from the midline. Neuron 10:409–426

Sepp KJ, Auld VJ (2003) Reciprocal interactions between neurons and glia are required for *Drosophila* peripheral nervous system development. J Neurosci 23:8221–8230

Silies S, Klämbt C (2011) Adhesion and signaling between neurons and glia cells in *Drosophila*. Curr Opin Neurobiol 21:11–16

Silies M, Yuva Y, Engelen D, Aho A, Stork T, Klämbt C (2007) Glial cell migration in the eye disc. J Neurosci 27:13130–13139

Snow PM, Patel NH, Harrelson AL, Goodman CS (1987) Neural-specific carbohydrate moiety shared by many surface glycoproteins in *Drosophila* and grasshopper embryos. J Neurosci 7:4137–4144

Stevenson PA, Kutsch W (1986) Basic circuitry of an adult-specific motor program completed with embryogenesis. Naturwissenschaften 73:741–743

Strausfeld NJ (2009) Brain organization and the origin of insects: an assessment. Proc R Soc B 276:1929–1937

Strauss R (2002) The central complex and the genetic dissection of locomotor behaviour. Curr Opin Neurobiol 12:633–638

Swales LS, Lane NJ (1985) Embyronic development of glial cells and their junctions in the locust central nervous system. J Neurosci 5:117–127

Takahashi DK, Vargas JR, Wilcox KS (2010) Increased coupling and altered glutamate transport currents in astrocytes following kainic-acid-induced status epilepticus. Neurobiol Dis 40:573–585

Tanaka M, Yamaguchi K, Tatsukawa T, Theis M, Willecke K, Itohara S (2008) Connexin43 and bergmann glial gap junctions in cerebellar function. Front Neurosci 2:225–233

Theiss C, Meller K (2002) Aluminum impairs gap junctional intercellular communication between astroglial cells in vitro. Cell Tissue Res 310:143–154

Tiemeyer M, Goodman CS (1996) Gliolectin is a novel carbohydrate binding protein expressed by a subset of glia in the embryonic *Drosophila* nervous system. Development 122:925–936

van der Hel WS, Notenboom RGE, Bos IWM, van Rijen PC, van Veelen CWM, de Graan PNE (2005) Reduced glutamine synthetase in hippocampal areas with neuron loss in temporal lobe epilepsy. Neurology 64:326–333

Vanhems E (1985) An in vitro autoradiographic study of gliogenesis in the embryonic locust brain. Dev Brain Res 23:269–275

Vasenkova I, Luginbuhl D, Chiba A (2006) Gliopodia extend the range of direct glia-neuron communication during the CNS development in *Drosophila*. Mol Cell Neurosci 31:123–130

Viktorin G, Riebli N, Popkova A, Giangrande A, Reichert H (2011) Multipotent neural stem cells generate glial cells of the central complex through transit amplifying intermediate progenitors in *Drosophila* brain development. Dev Biol 356:553–565

Weber PA, Chang HC, Spaeth KE, Nitsche JM, Nicholson BJ (2004) The permeability of gap junction channels to probes of different size is dependent on connexin composition and permeant-pore affinities. Biophys J 87:958–973

Wedler FC, Horn BR (1976) Catalytic mechanisms of glutamine synthetase enzymes. J Biol Chem 251:7530–7538

Weingart R, Bukauskas FF (1998) Long-chanin n-alkanols and arachidonic acid interfere with the Vm-sensitive gating mechanisms of gap junction channels. Eur J Physiol 435:310–319

Wilcox MJ (1994) Structure and function of gap junctions in the photoreceptor axon terminals of the fly. Adv Chem 235:225–243

Williams JLD (1975) Anatomical studies of the insect central nervous system: a ground-plan of the midbrain and an introduction to the central complex in the locust, *Schistocerca gregaria* (Orthoptera). J Zool Lond 176:67–86

Young JM, Armstrong JD (2010a) Structure of the adult central complex in *Drosophila*: organization of distinct neuronal subsets. J Comp Neurol 518:1500–1524

Young JM, Armstrong JD (2010b) Building the central complex in *Drosophila*: the generation and development of distinct subsets. J Comp Neurol 518:1525–1541

Zahs KR, Newman E (1997) Asymmetric gap junctional coupling between glial cells in the rat retina. Glia 20:10–22